

A new method for wideband characterization of resonator-based sensing platforms

Farasat Munir, Adam Wathen, and William D. Hunt

Citation: *Rev. Sci. Instrum.* **82**, 035119 (2011); doi: 10.1063/1.3567005

View online: <http://dx.doi.org/10.1063/1.3567005>

View Table of Contents: <http://rsi.aip.org/resource/1/RSINAK/v82/i3>

Published by the [American Institute of Physics](#).

Related Articles

Intrinsically tunable 0.67BiFeO₃-0.33BaTiO₃ thin film bulk acoustic wave resonators

Appl. Phys. Lett. **101**, 232903 (2012)

Interpreting picosecond acoustics in the case of low interface stiffness

Rev. Sci. Instrum. **83**, 114902 (2012)

Acoustic filter based on Helmholtz resonator array

Appl. Phys. Lett. **101**, 051907 (2012)

Tunable coupled surface acoustic cavities

Appl. Phys. Lett. **100**, 261904 (2012)

Extremely low-loss acoustic phonons in a quartz bulk acoustic wave resonator at millikelvin temperature

Appl. Phys. Lett. **100**, 243504 (2012)

Additional information on Rev. Sci. Instrum.

Journal Homepage: <http://rsi.aip.org>

Journal Information: http://rsi.aip.org/about/about_the_journal

Top downloads: http://rsi.aip.org/features/most_downloaded

Information for Authors: <http://rsi.aip.org/authors>

ADVERTISEMENT



AIPAdvances

Now Indexed in
Thomson Reuters
Databases

Explore AIP's open access journal:

- Rapid publication
- Article-level metrics
- Post-publication rating and commenting

A new method for wideband characterization of resonator-based sensing platforms

Farasat Munir, Adam Wathen, and William D. Hunt

School of Electrical and Computer Engineering, Georgia Institute of Technology, 791 Atlantic Dr., Atlanta, Georgia 30332, USA

(Received 15 January 2011; accepted 12 February 2011; published online 29 March 2011)

A new approach to the electronic instrumentation for extracting data from resonator-based sensing devices (e.g., microelectromechanical, piezoelectric, electrochemical, and acoustic) is suggested and demonstrated here. Traditionally, oscillator-based circuitry is employed to monitor shift in the resonance frequency of the resonator. These circuits give a single point measurement at the frequency where the oscillation criterion is met. However, the resonator response itself is broadband and contains much more information than a single point measurement. Here, we present a method for the broadband characterization of a resonator using white noise as an excitation signal. The resonator is used in a two-port filter configuration, and the resonator output is subjected to frequency spectrum analysis. The result is a wideband spectral map analogous to the magnitude of the S_{21} parameters of a conventional filter. Compared to other sources for broadband excitation (e.g., frequency chirp, multisine, or narrow time domain pulse), the white noise source requires no design of the input signal and is readily available for very wide bandwidths (1 MHz–3 GHz). Moreover, it offers simplicity in circuit design as it does not require precise impedance matching; whereas such requirements are very strict for oscillator-based circuit systems, and can be difficult to fulfill. This results in a measurement system that does not require calibration, which is a significant advantage over oscillator circuits. Simulation results are first presented for verification of the proposed system, followed by measurement results with a prototype implementation. A 434 MHz surface acoustic wave (SAW) resonator and a 5 MHz quartz crystal microbalance (QCM) are measured using the proposed method, and the results are compared to measurements taken by a conventional bench-top network analyzer. Maximum relative differences in the measured resonance frequencies of the SAW and QCM resonators are 0.0004% and 0.002%, respectively. The ability to track a changing sensor response is demonstrated by inducing temperature variations and measuring resonance frequency simultaneously using the proposed technique in parallel with a network analyzer. The relative difference between the two measurements is about 5.53 ppm, highlighting the impressive accuracy of the proposed system. Using commercially available digital signal processors (DSPs), we believe that this technique can be implemented as a system-on-a-chip solution resulting in a very low cost, easy to use, portable, and customizable sensing system. In addition, given the simplicity of the signal and circuit design, and its immunity to other common interface concerns (injection locking, oscillator interference, and drift, etc.), this method is better suited to accommodating array-based systems.

© 2011 American Institute of Physics. [doi:[10.1063/1.3567005](https://doi.org/10.1063/1.3567005)]

I. INTRODUCTION AND BACKGROUND

Resonator-based sensing platforms have been widely studied for use in chemical and biological applications. A notable historic example is the development of the quartz crystal microbalance (QCM) for mass sensing first reported by Sauerbrey in 1959.¹ Since then, a variety of other types of resonators have been developed, taking advantage of microelectronic fabrication techniques. Examples of more modern resonators include membrane resonators,² cantilever resonators,^{3–5} and high frequency surface and bulk acoustic wave (SAW and BAW) devices.^{6–8}

The sensing functionality is achieved by coating the resonator with a chemically sensitive or selective layer. A change in physical properties of this layer due to the sensing event affects the resonator response. An electronic system is required to interface with the resonator and track the changing resonator response. The response parameters (e.g., resonance

frequency) are further converted to physical parameters (e.g., mass density and viscosity) of the thin film coating by using equivalent circuit models.^{9,10}

Traditionally, oscillator circuits are used for monitoring the shift of the resonance frequency, f_0 , of the resonator. The resonator is employed in the feedback loop of the oscillator as a frequency-determining element. These circuits provide only a single point measurement at the frequency where the oscillation criterion is met. However, the resonator response itself is broadband and contains much more information than a single point measurement. As an example, resonators operating in liquid phase experience a strongly damped Q as compared to gaseous phase. Extreme phase and circuit stability are required to obtain stable single frequency oscillation.¹¹ Hence, various modifications to simple oscillator circuits are reported which use automatic gain control^{10,12} or parallel capacitance compensation techniques.¹³ It is very difficult to

maintain the accuracy of the measurements under reduced Q conditions and, therefore, a careful calibration of the oscillator circuit is required. This calibration in oscillator based circuits may require expensive instruments such as network analyzers.¹⁰ Phase locked loop (PLL) based techniques have been proposed^{14–16} to overcome these issues but are relatively more complex and also require calibration. This calibration in PLL based circuits is achieved by employing additional reference phase locked loops, thus resulting in manifold increase in circuit complexity. Another type of interface circuit relies on impulse excitation of the resonator. A popular example is the ring-down technique.¹⁷ In addition to the resonance frequency, this method does provide an additional measurement point (energy dissipation, D , or quality factor, $Q = 1/D$), but still relies on oscillator circuitry and suffers from the same problems previously mentioned.

Measurement of the shift in the resonance frequency and quality factor is not always enough for complete determination of the physical parameters of the tested sample. In particular, for biosensors operating in liquid loading conditions, there are more than two unknown physical parameters (such as mass density, shear modulus, film thickness) of the sample.¹⁸ Therefore, a complete characterization of the impedance spectrum is useful, which can be only performed using network analyzers that are sophisticated, bulky, and expensive. Hence, they are not suitable for *in situ* techniques. Systems operating on the principle of network analysis, but with smaller and less expensive electronics, have been developed for quartz crystal resonators.^{19,20} Unlike network analyzers, they operate in a narrow range around the resonance frequency. As an alternative to impedance spectra, systems measuring a “voltage transfer function,” dependent on sensor-impedance, have been reported; however, the transfer function method requires further fitting to application-specific models to extract load data.²¹

Simultaneous detection of multiple biomarkers requires multielement sensor array systems. Such a system is very useful for screening of diseases like cancer or sepsis where single biomarker detection is not conclusive.^{22,23} Arrays of resonators have some unique electrical interface circuit requirements. In particular, for oscillator-based circuit designs, each amplifier–resonator pair must be designed separately to measure the shift in resonance frequency. However, each individual oscillator loop in the array is prone to interference and frequency pulling effects from neighboring resonators in the array. Therefore, it is difficult to extract and compare the orthogonal responses of individual resonators.

Excitation of a resonator with a sufficiently wideband signal gives an output that will contain only the filtered frequencies representative of the transfer function of the resonator. Previously, different types of wideband excitation signals have been used with resonators (i.e., multifrequency chirp and narrow time domain impulse).^{24,25} Each of these signals requires careful design of the signal itself as well as the circuit layout for the specific type, resonance frequency, and bandwidth of the resonator. These signals have their individual limitations for use with resonators: the chirped signal requires larger measurement time and the time domain pulse excitation signal is not well suited to very high Q



FIG. 1. (Color online) Spectral analysis of noise excited resonator.

resonators²⁵ such as a QCM ($Q \sim 30,000$). Moreover, the response of reduced Q resonators (as experienced under liquid loading conditions) spans a larger bandwidth. The time domain input pulse, then, must be very narrow in time and, correspondingly, its power is dispersed over a larger bandwidth. This will reduce the power at the resonance frequency down to a level which may fail to excite the resonance.²⁵

Another wideband signal is a multisine signal which is commonly used for frequency domain system identification and characterization. Its application to resonant systems has not been reported. However, the circuit design for multisine generation is very complicated, especially at high frequencies.²⁶ A multisine signal provides wideband excitation but its spectrum is discrete and will therefore be resolution limited and ill-suited for high Q resonators.

In this paper, we attempt to circumvent these issues and present an argument for and simulation and experimental results of a new approach to the electronic instrumentation for extracting data from resonator-based sensing devices based on white noise excitation. An electromechanical resonator is used in a two-port filter configuration and its output is then subjected to frequency domain spectral analysis. This proposed method is shown schematically in Fig. 1. We further show that it offers a very simplistic interface design with several advantages over conventional methods of parameter extraction and tracking. The white noise source requires no design of the input signal and is readily available commercially for very wide bandwidths (1 MHz–3 GHz). Moreover, it offers simplicity in circuit design, as it does not require precise impedance matching; whereas such requirements are very strict for oscillator circuit systems, and are hard to fulfill. This results in a measurement system that does not require calibration, which is a significant advantage over oscillator circuits. The measurement output of this method is experimentally compared to that of a bench-top network analyzer and is shown to agree within 0.002%. Given the simplicity in the signal and circuit design, and its immunity to other common interface concerns (injection locking, oscillator interference, drift, etc.), this method is better suited to accommodating array-based systems.

II. THEORETICAL UNDERPINNINGS AND SIMULATION RESULTS

In deterministic signal scenarios, the input and output of a linear system are directly related through the transfer function. In the case of the excitation of linear systems with stochastic inputs, such direct characterization does not exist. The white noise input signal proposed here can be assumed wide-sense stationary. The second-order moments of such a signal (such as autocorrelation) can be used to characterize

the system transfer function. The Fourier transform of the autocorrelation gives the power spectral density (PSD), which is used for frequency domain characterization. For a random input signal, the input and output power density spectrums of the resonator are related a

$$\Gamma_{yy} = \Gamma_{xx}|H(F)|^2 \quad (1)$$

where, Γ_{yy} is the output PSD, Γ_{xx} is the input PSD, $|H(F)|$ is the resonator transfer function in the frequency domain, $|H(F)|^2$ is thus the energy density spectrum of the resonator response. If the input is a white noise signal with power σ_x^2 , then we have

$$\Gamma_{yy} = \sigma_x^2 |H(F)|^2. \quad (2)$$

Thus, for white noise, the output PSD is proportional to the energy density spectrum of the resonator frequency response scaled by the power of input noise. The output, then, gives us a measure of the magnitude of the frequency response of the resonator. We cannot measure the phase of the resonator response with this method, which is very essential for oscillator based interface methods. The phase measurement, though holds a much lesser significance here, because the frequency response measured by this method can give a direct measure of the resonance frequency, f_r , and the half-band-half-width (HBHW), bandwidth of the resonator. Conventionally, these two parameters are used for characterizing the resonator, and are measured using network analyzers. It has been shown by various groups for acoustic as well as MEMS resonators that the viscoelastic properties of the surface perturbation sample can be deduced by analyzing the resonance frequency and bandwidth.^{21,27–31} Resonance frequency and dissipation (measured by oscillator based interface circuits coupled with impulse excitation) have also been extensively used to interpret the viscoelastic properties of the surface coating layer and the tested sample.^{32,33} Both of these methods are equivalent as Johannsmann has given a relation that describes dissipation, D , in terms of the HBHW bandwidth.³⁴ Furthermore, convergence relationships of dissipation analysis and the analysis based on Δf and ΔHBHW , have also been reported.³⁵

The proposed method described here gives not only information about f_r and Γ , but also the wide-bandwidth transfer function of the resonator (with a much simpler setup than a network analyzer). Potentially, this could offer more useful information than just relying on the f_r and Γ .

The setup of Fig. 1 was simulated using SIMULINK® software by MathWorks®. The simulation setup is shown in Fig. 2.

The “white noise” block generates a signal with a uniform frequency distribution as an input to the resonator. To model the resonator response accurately in the simulation,

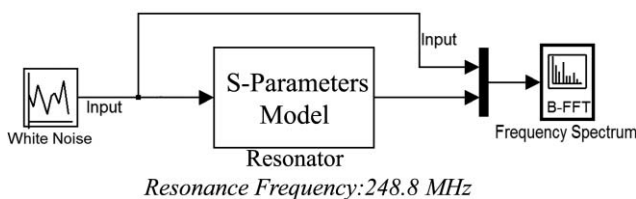


FIG. 2. Setup for simulating noise excited response of a resonator.

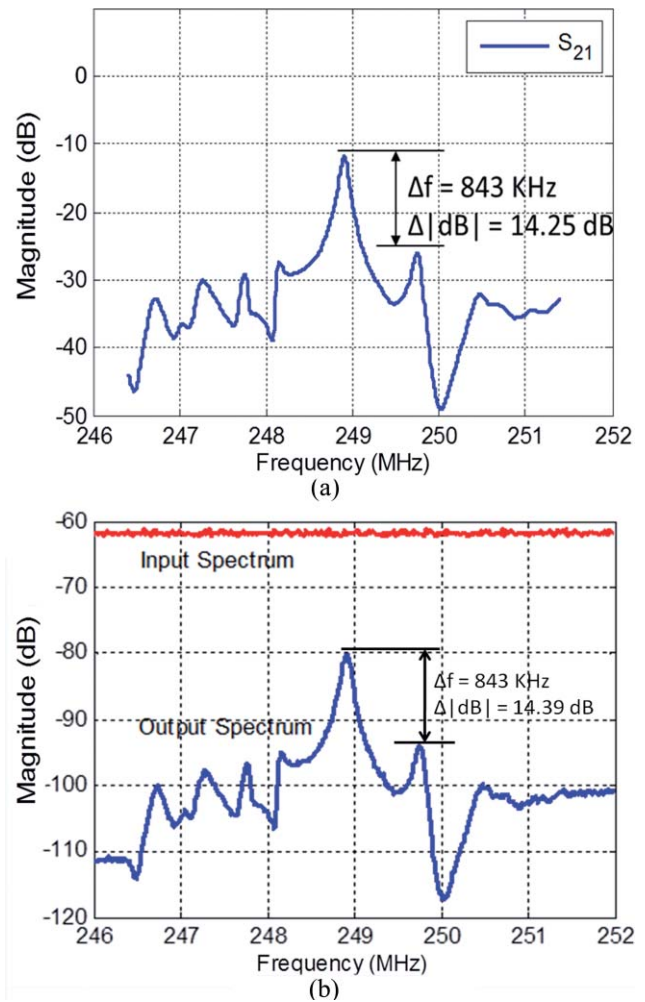


FIG. 3. (Color online) (a) Measured S-parameters of a SAW resonator. (b) Simulated FFT scope output showing both the input noise spectrum and the output of the resonator.

a measured S-parameters file of an actual SAW resonator is used. The FFT scope is used for power spectrum density analysis. The results are shown in Fig. 3. Notice that in this simulation setup, we used a two-port resonator and the output frequency response is similar to the S21 response. However, one-port devices can also be used in this technique by employing them as a through element in a two-port measurement system. The results in Fig. 3 are for an FFT of 1024 points. We did the simulation for an FFT size of 256, 512, 1024, and 2048. The relative error between the S21 and FFT output decreased with increasing FFT size. However, there was minimal improvement between 1024 and 2048 point FFT. We expect that the FFT size required for a minimal relative error is dependent on the resonator quality factor and the particular sensing application. The purpose of presenting this simulation is to give a proof-of-concept for the proposed method, which is clearly demonstrated by the results shown in Fig. 3. Next, we demonstrate the scalability of the proposed method to resonator arrays.

Figure 4(a) shows the setup for exciting a two-element resonator array simultaneously with a single noise source. The resonators are again modeled using their S-parameters files with their individual resonance peaks (in the S21

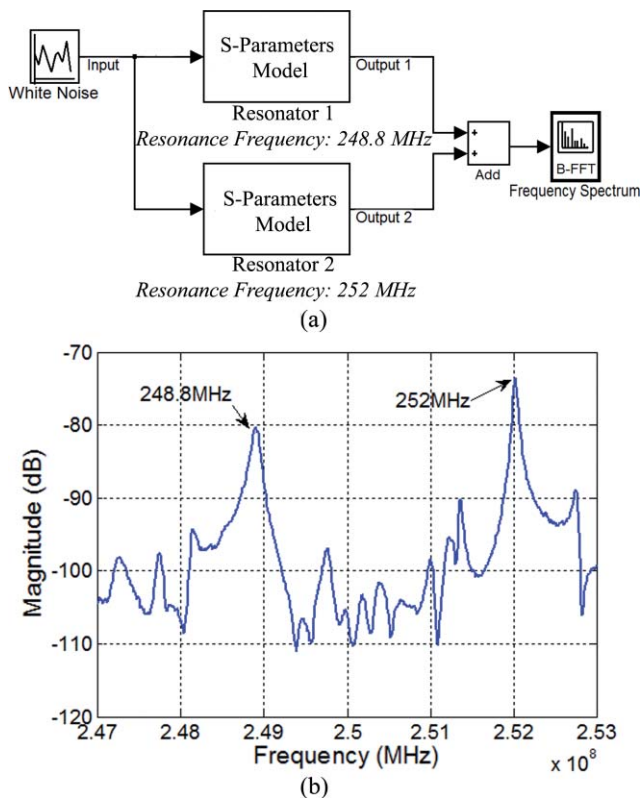


FIG. 4. (Color online) (a) Simulation setup for two-element resonator array. (b) The noise excited spectral output of a two-element resonator array.

response) at 248.8 and 252 MHz. The simulated FFT of the combined output shows that the individual responses of each resonator element are reproduced fairly accurately in the spectral output. Based on these simulation results, we suggest that the proposed method can be easily extended to resonator arrays. This method provides a significant advantage over all other methods for array systems by eliminating the need for multiple input sources or a switching method between array elements. However, it requires that the resonance frequency of each element in the resonator array is offset from the other elements in the array. Implementing such an array system has been reported by Yang *et al.*²⁴

III. MEASUREMENT RESULTS

To further investigate the proposed system, we built a prototype using a surface mount noise source, SMN-7114-C2A by Micronetics® Inc. This noise source excites a resonator and the output spectrum is measured using an E4404B Agilent Spectrum Analyzer (SPA). The noise source and its frequency spectrum are shown in Fig. 5(a). The prototype setup is shown in Fig. 5(b). Using this setup, we measured two different types of resonators—a 434 MHz SAW resonator and a 5 MHz QCM.

A. SAW resonator

We measured a 434 MHz SAW resonator with the prototype setup shown in Fig. 5(b). A comparison of the SAW resonator output as measured by the SPA and as measured by the Vector Network Analyzer (VNA) is shown in Fig. 6. It is

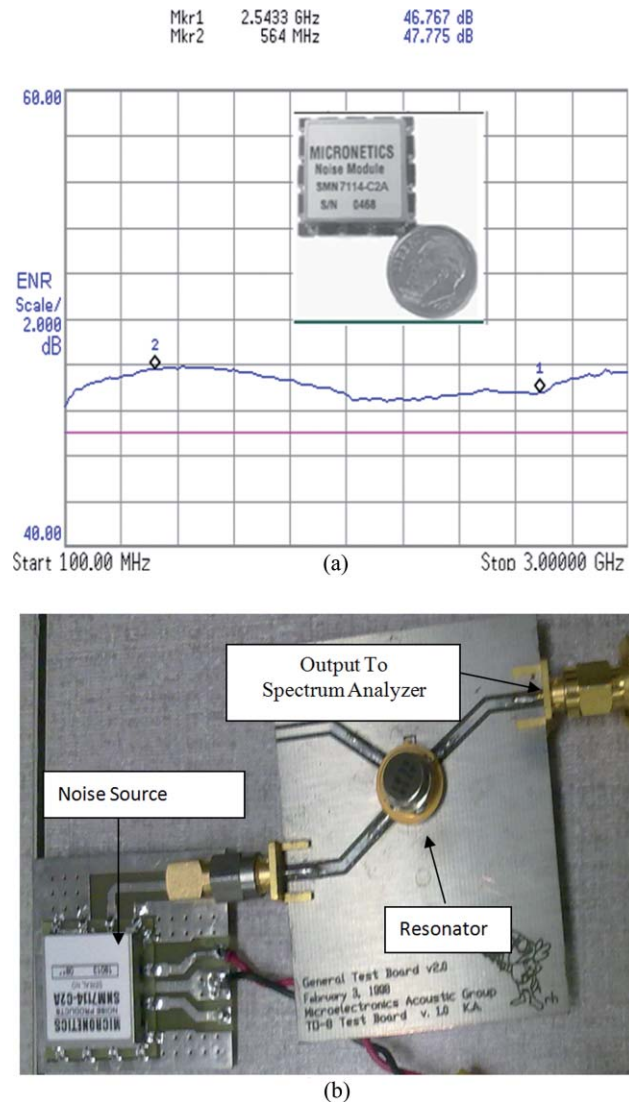
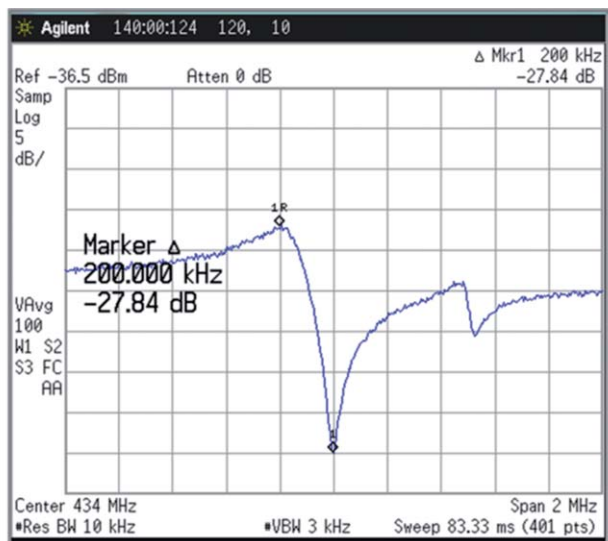
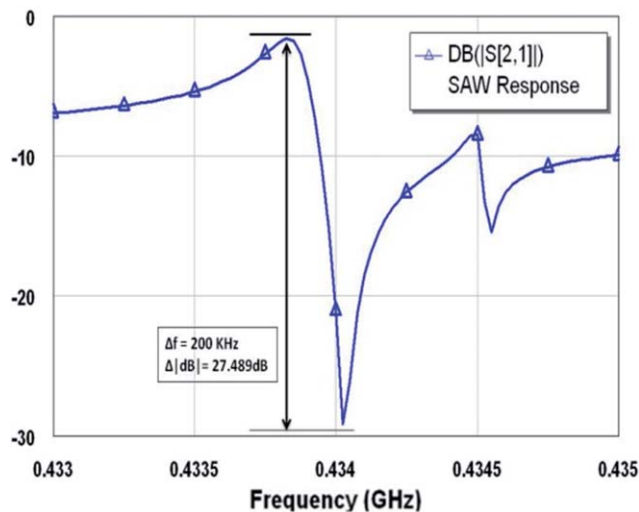


FIG. 5. (Color online) (a) SMN-7114-C2A noise source and its spectrum. (b) Prototype setup snapshot.

evident that both responses are comparable in frequency content. The characteristic resonance peaks are replicated at the same frequencies, and the relative strengths of frequency content are preserved and have been explicitly marked. It should be noted that the measurements with the proposed method are done without any calibration. The remarkable accuracy of the proposed system is further highlighted in Fig. 7, where both responses are plotted in the same graph. There is no scaling employed on frequency or magnitude axis, but both responses are plotted after subtracting the respective mean power levels. The frequency resolution for VNA measurements and for SPA measurements is 3 and 10 kHz, respectively. The resonance frequencies (taken as the frequency at the minimum point in the S21 amplitude) measured by VNA and SPA are 433.996875 and 434.000000 MHz, respectively. This gives a relative difference of about 0.0004%. The mean amplitude difference over the entire bandwidth of measurement, between the two methods is 0.3 dB with a variance of 0.09 dB. Further accuracy can also be obtained by improving the frequency resolution of the SPA, but at the cost of increased measurement time.



(a)



(b)

FIG. 6. (Color online) Noise excited resonator output. (a) Measured by a spectrum analyzer. (b) Measured by a vector network analyzer.

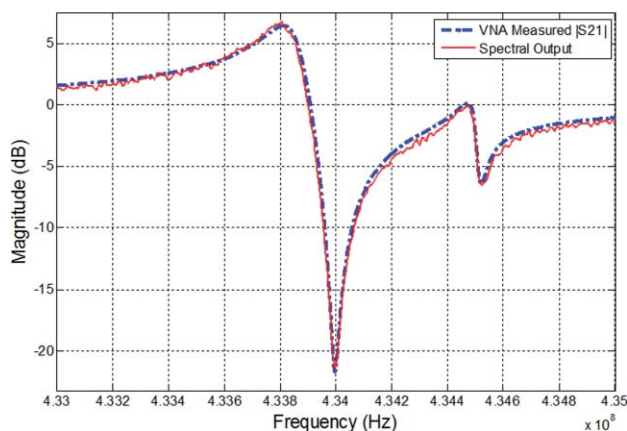


FIG. 7. (Color online) Measured responses of SAW resonator by VNA and the proposed method after mean level subtraction.

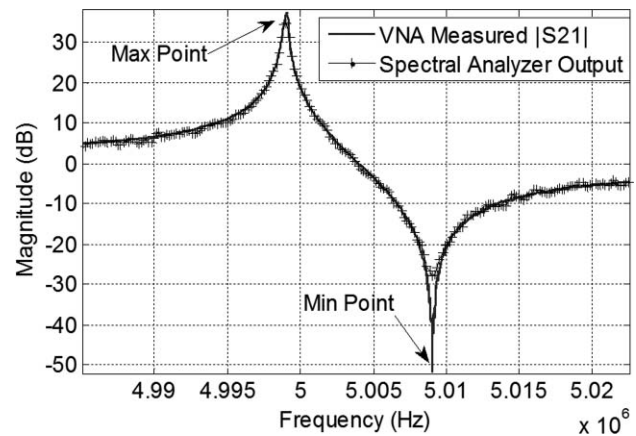


FIG. 8. Measured responses of QCM by the VNA and the proposed method after mean level subtraction.

B. Quartz crystal microbalance

The same circuit setup shown in Fig. 5(b) without any modification can be used for measuring low frequency or high frequency resonators, as well as one-port resonators. However, one-port resonators will be needed to plug into the two-port circuit setup as through elements. To demonstrate these properties of the proposed system, we measured a 5 MHz QCM (a very low frequency, one-port resonator) with the same circuit that was used for the SAW resonator mentioned above. We measured the two-port S-parameters of the QCM with the VNA as well as with our proposed method. Figure 8 shows the two responses in a single plot with the mean power level for each response subtracted from its respective response.

Here, we present a comparison of QCM measurement with the two methods. There are two distinct points in the QCM response which corresponds to the maximum amplitude point (Max Point) and minimum amplitude point (Min Point). Each of these could be considered a measure of resonance frequency. At the maximum, the resonance frequencies measured by the VNA and the SPA are 4.9991 and 4.9990 MHz, respectively. This gives a relative difference in resonance frequencies of about 0.002%. The mean amplitude difference between the two methods (over the entire bandwidth of measurement) is 0.58 dB with a variance of 1.4 dB. However, these numbers are misleading because the SPA response is not following the VNA-measured results in the negative dip at minimum. This error is due to the fact that the QCM response has a very large dynamic range (~ 80 – 90 dB), which takes the negative dip well below the noise floor of the SPA. Therefore, the QCM response is truncated at the negative dip as it has approached the noise floor of the SPA (~ -124 dBm). This problem can be taken care of by properly amplifying the input noise signal level to raise the output of the resonator well above the SPA noise floor.

C. Frequency tracking ability

We measured the temperature curve of the SAW device with both a VNA and the proposed method. The temperature

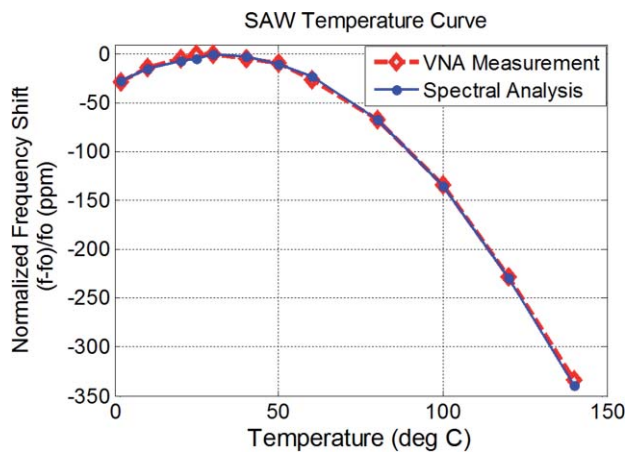


FIG. 9. (Color online) Temperature curve measurement of SAW device with VNA and with noise-excited spectral measurement.

was varied from 0 to 100 °C and at each temperature point the devices were allowed to settle for 2 min. The changes in device response with changing temperature were tracked by measuring the maximum amplitude point in the frequency response obtained by the spectral analyzer and in the IS211 response measured by the VNA. An important detail to note here is that VNA measurements were taken after a tedious two-port calibration of the VNA, whereas the measurements with our proposed method were taken without any calibration. Results are shown in Fig. 9. The temperature curves measured by both techniques are in agreement with a maximum difference of 5.53 ppm. This experiment demonstrates the ability of the proposed method to accurately track changes in the frequency response of the resonator.

IV. DISCUSSION

The proposed system described above gives a wideband response of the resonator with a very simple setup. The wide-

band frequency response has more information than just the measurement of resonance frequency and bandwidths. This extra information could be potentially useful for extraction of the physical parameters of the surface load. It is extremely difficult to find and track the resonance frequency shifts of the resonator when heavily loaded by liquid. The oscillations may even fail to occur due to high damping. Therefore, under heavy liquid loading conditions the proposed method has an advantage over other methods as it is not just a single point measurement. Moreover, because of noise being used as the input signal, significant advantages are obtained over conventional single frequency excitation systems such as oscillators. Circuit design for the proposed method is relatively independent of resonance frequency variations. Hence, the same circuit designed for a particular center frequency may be used for a very large bandwidth around the center frequency. We demonstrated the use of same circuit for 5 and 434 MHz devices without using any calibration for either device. The proposed method is relatively immune to parasitic effects compared to oscillator-based systems. It is also immune to background noise fluctuations which appear as a jitter in the oscillator-based systems and result in limited frequency resolution. Wideband white noise has a continuous frequency spectrum and hence, the resolution is, theoretically, not limited. In practice, though the resolution will be limited by the sampling rate of the analog to digital converter (ADC), and the FFT resolution.

There are some additional benefits for noise excitation of resonator arrays. It does not require individual circuits tuned for individual sensors. A single input source drives all the sensors simultaneously with no switches required (switching circuits introduce an additional complexity at high frequencies). In our proposed method, each resonator outputs its own frequency response and is not in an oscillator configuration where loop dynamics can lock onto external signal (from a neighboring resonator) injected into the loop.³⁶ Therefore, it will be immune to interference from neighboring resonators (Table I).

TABLE I. Summarized comparison of oscillator based systems and the proposed method.

	Oscillator-based interface circuitry for resonators	Noise excited spectral analysis of resonators
Measured information content	<ul style="list-style-type: none"> • Gives a single point measurement of the resonance frequency only 	<ul style="list-style-type: none"> • Gives a wideband frequency response, holding much more information than just the resonance frequency
Circuit design	<ul style="list-style-type: none"> • Strict requirements of phase stability • Requires precise impedance matching • Circuit design requires modification with the change in resonance frequency • Phase noise appears as jitter and limits the frequency resolution 	<ul style="list-style-type: none"> • No phase compensation requirements • Tolerant to mismatch over a broadband • Same circuit can operate over a wide range of resonance frequencies • Immune to phase noise and limited in frequency resolution only by FFT size
Reduced Q conditions	<ul style="list-style-type: none"> • Difficult to excite oscillations • Requires complex circuit modifications for accurate measurements 	<ul style="list-style-type: none"> • No Oscillatory behavior needed • Same setup can be used for both reduced Q and high Q conditions
Array systems	<ul style="list-style-type: none"> • Requires individual circuit tuned for individual elements of the array • Each element is prone to interference (due to injection locking) from neighboring resonators in the array 	<ul style="list-style-type: none"> • Array is excited as a whole and hence does not require individual circuit for each element • No oscillator loops are involved and hence interference from neighboring elements is not a concern

V. CONCLUSION

We have presented a novel method to measure and track a resonator's response and extract its characterization parameters. This method measures the wideband frequency response of the resonator with a much simpler setup compared to conventional methods. We have suggested and demonstrated the use of a white noise signal as a viable signal for broadband excitation of resonator-based sensing platforms. We have also established, through simulation and prototype measurements, the feasibility of the proposed method. The accuracy and speed of the system can be further improved by FFT-based digital implementation of the spectral analysis system. This will allow for a low-cost and compact solution in the form of a system on a chip.

ACKNOWLEDGMENTS

This work was supported in part by the V Foundation and by the National Cancer Institute (NCI) (Grant No. 2106AZX). The authors also wish to thank Mohammad Omer for several helpful discussions regarding the MATLAB® simulations.

- ¹G. Z. Sauerbrey, *Physik* **155**, 206 (1959).
- ²R. Abdolvand, H. Zhili, and F. Ayazi, in *Proceedings of the 5th IEEE Conference on Sensors*, 1297–1300, 2006.
- ³R. Raiteri, M. Grattarola, H. J. Butt, and P. Skladal, *Sens. Actuators B* **79**(2–3), 115 (2001).
- ⁴T. Liu, J. Tang, M. Han, and L. Jiang, *Biochem. Biophys. Res. Commun.* **304**(1), 98 (2003).
- ⁵J. Verd, A. Uranga, G. Abadal, J. L. Teva, F. Torres, J. L. Lopez, E. Perez-Murano, J. Esteve, and N. Barniol, *IEEE Electron Device Lett.* **29**(2), 146 (2008).
- ⁶S. Rey-Mermet, R. Lanz, and P. Muralt, *Sen. Actuators B* **114**(2), 681 (2006).
- ⁷F. Bender, P. Roach, A. Tsortos, G. Papadakis, M. I. Newton, G. McHale, and E. Gizeli, *Meas. Sci. Technol.* **20**(12), 124011 (2009).
- ⁸D. D. Stubbs, L. Sang-Hun, and W. D. Hunt, in *Proceedings of IEEE Conference on Sensors* **1**, 335–338, 2002.
- ⁹R. Lucklum and P. Hauptmann, *Electrochim. Acta* **45**(22–23), 3907 (2000).
- ¹⁰R. Borngraber, J. Schroder, R. Lucklum, and P. Hauptmann, *IEEE Trans. Ultrason. Eng.* **49**(9), 1254 (2002).
- ¹¹R. Lucklum and F. Eichelbaum, in *Piezoelectric Sensors*, edited by A. Janshoff and C. Steinem (Springer, Berlin, Heidelberg, 2007), vol. 5, pp. 3–47.
- ¹²C. Chagnard, P. Gilbert, A. N. Watkins, T. Beeler, and D. W. Paul, *Sen. Actuators B* **32**(2), 129 (1996).
- ¹³R. Behrends and U. Kaatz, *Meas. Sci. Technol.* **12**(4), 519 (2001).
- ¹⁴A. Arnau, T. Sogorb, and Y. Jimenez, *Rev. Sci. Instrum.* **71**(6), 2563 (2000).
- ¹⁵D. Rocha, V. Ferrari, and B. Jakoby, in *Proceedings of the IEEE on Sensors*, **1**, 32–35, 2004.
- ¹⁶T. Nakamoto and T. Kobayashi, *IEEE Trans. Ultrason. Eng.* **41**(6), 806 (1994).
- ¹⁷M. Rodahl and B. Kasemo, *Rev. Sci. Instrum.* **67**(9), 3238 (1996).
- ¹⁸A. R. Hillman, A. Jackson, and S. J. Martin, *Anal. Chem.* **73**(3), 540 (2001).
- ¹⁹J. Schroder, R. Borngraber, R. Lucklum, and P. Hauptmann, *Rev. Sci. Instrum.* **72**(6), 2750 (2001).
- ²⁰R. Schnitzer, C. Reiter, K. C. Harms, E. Benes, and M. Groschl, *IEEE Sens. J.* **6**(5), 1314 (2006).
- ²¹F. Eggers and T. Funck, *J. Phys. E: J. Sci. Instrum.* **20**(5), 523 (1987).
- ²²K. R. Kozak, F. Su, J. P. Whitelegge, K. Faull, S. Reddy, and R. Farias-Eisner, *Proteomics* **5**(17), 4589 (2005).
- ²³D. D. Taylor, S. Atay, D. S. Metzinger, and C. Gercel-Taylor, *Gynecol. Oncol.* **116**(2), 213 (2010).
- ²⁴Y. T. Yang, C. Callegari, X. L. Feng, K. L. Ekinci, and M. L. Roukes, *Nano Lett.* **6**(4), 583 (2006).
- ²⁵R. P. Wali, P. R. Wilkinson, S. P. Eaimkhong, J. Hernando-Garcia, J. L. Sanchez-Rojas, A. Ababneh, and J. K. Gimzewski, *Sens. Actuators B* **147**(2), 508 (2010).
- ²⁶N. B. Carvalho, J. C. Pedro, and J. P. Martins, *IEEE Trans. Microwave Theory Tech.* **54**(6), 2659 (2006).
- ²⁷B. Du and D. Johannsmann, *Langmuir* **20**(7), 2809 (2004).
- ²⁸H. L. Bandey, S. J. Martin, R. W. Cernosek, and A. R. Hillman, *Anal. Chem.* **71**(11), 2205 (1999).
- ²⁹R. Lucklum, C. Behling, R. W. Cernosek, and S. J. Martin, *J. Phys. D: Appl. Phys.* **30**(3), 346 (1997).
- ³⁰R. Etchenique and A. D. Weisz, *J. Appl. Phys.* **86**(4), 1994 (1999).
- ³¹D. Johannsmann, *J. Appl. Phys.* **89**(11), 6356 (2001).
- ³²M. Rodahl, F. Hook, A. Krozer, P. Brzezinski, and B. Kasemo, *Rev. Sci. Instrum.* **66**(7), 3924 (1995).
- ³³M. V. Voinova, M. Rodahl, M. Jonson, and B. Kasemo, *Phys. Scr.* **59**(5), 391 (1999).
- ³⁴D. Johannsmann, in *Piezoelectric Sensors*, edited by A. Janshoff and C. Steinem (Springer, Berlin, Heidelberg, 2007), vol. 5, pp. 49–109.
- ³⁵Y. Zhang, B. Du, X. Chen, and H. Ma, *Anal. Chem.* **81**(2), 642–648 (2009).
- ³⁶P. J. Edmonson, P. M. Smith, and C. K. Campbell, *Ultrasonics, Ferroelectrics and Frequency Control, IEEE Transactions* **39**(5), 631–637 (1992).